Journal of Material Cycles and Waste Management (2020) 22:228–239
https://doi.org/10.1007/s10163-019-00933-2

ORIGINAL ARTICLE

PSO–ANN-based prediction of cobalt leaching rate from waste lithium-ion batteries

Hossein Ebrahimzade[1] · Gholam Reza Khayati[2] · Mahin Schaffie[3]

Received: 23 January 2019 / Accepted: 10 October 2019 / Published online: 26 October 2019
© Springer Japan KK, part of Springer Nature 2019

Abstract
Leaching is a complex solid–liquid reaction which has an important influence on the recovery efficiency of the spent lithium-ion batteries (LIBs). Therefore, it is of significant importance to utilize an appropriate technique to predict the effect of operating parameters on the optimized recovery rate. In the present study, a combined method of the artificial neural network (ANN) and particle swarm optimization algorithm (PSO) was used as a model to predict the leaching efficiency of cobalt from spent LIBs. To find the dependency of the leached percentage of cobalt on the operational parameters as model inputs, 42 repeatable numerous experiments are performed using H_2SO_4 in the presence of H_2O_2. It was found that the proposed model can be a useful technique in the demonstration of the nonlinear relationship between the leaching efficiency and the process parameters. The performance of PSO–ANN models was validated by statistical thresholds and compared with those of common ANN technique. Moreover, it was found that the pulp density of the leaching solution and the concentration of sulfuric acid were the most important reaction parameters of the spent LIBs recovery, respectively.

Keywords Spent Li-ion batteries · Leaching · Reaction parameters · Cobalt · PSO–ANN algorithm

Introduction

Understanding the influence of reaction parameters on the leaching efficiency is essential for process design and optimized recovery of the main components from waste lithium-ion batteries. Recently, the application of secondary ion batteries as an electrochemical power source is extensively enhanced especially in the fields of portable electronics due to their unique characteristics. LIBs are widely used in cellular phones, laptops, and other modern-life appliances by virtue of their outstanding properties. It is estimated that only in the China market in 2020, the weight and the quantity of LIBs will reach 500 tons and 25 billion units, respectively. The increasing application of LIBs inevitably leads to produce a lot of spent LIBs and subsequently causing environmental problems and resource depletion worldwide. Therefore, comprehensive studies seem to be essential for the maximum recovery of valuable elements from spent LIBs in a useful manner to avoid ecological pollution in addition to recycle alternative resources of valuable metals [1].

Different hydrometallurgical methods have been widely developed to recover valuable metals from the spent LIBs [2–7]. On the other hand, the leaching process is the main and conventional step of the sustainable metal recovery and subsequently accurate process design requires the detailed study and the proper prediction of the corresponding reactions. Waste LIBs leaching process is mainly carried out using mineral or organic acids and in some cases with reducing reagents (e.g. H_2O_2, $NaHSO_3$) [1]. In general, the efficiency of leaching with mineral acids is higher than that of organic acids. Sulfuric acid is preferred in industrial processes owing to high leaching efficiency (especially at high *S/L* ratios), less corrosion of equipment's, and the absence of toxic gases such as Cl_2, NO_x, etc. The leaching is a complex nonlinear process which cannot be modeled accurately through linear regression or function fitting approximation methods. Accordingly, the optimal recovery of the valuable

✉ Hossein Ebrahimzade
nanoibrahimzade@gmail.com

[1] Mineral Industries Research Center (MIRC), Shahid Bahonar University of Kerman, PO Box No. 76135-133, Kerman, Iran

[2] Department of Materials Science and Engineering, Shahid Bahonar University of Kerman, PO Box No. 76135-133 Kerman, Iran

[3] Department of Chemical Engineering, Shahid Bahonar University of Kerman, PO Box No. 76135-133, Kerman, Iran

elements (Co, Li) by leaching of spent LIBs is one of the most effective features that determines whether recovery of spent LIBs in a given time frame can be used for industrial purposes. In view of the leaching process complexity importance, it seems to be necessary to employ advanced techniques for comprehensive study as well as the estimation of the maximum recovery of the spent LIBs main metals.

Owing to their widespread applications and their potential to solve nonlinear problems, artificial neural networks (ANNs) are one of the advanced and effective findings which assist to figure out a numerical quantification of the various physicochemical phenomena. ANN can model the processes by pattern training, instead of completely identifying the point by point physical qualities and mathematical state function of the procedure. In comparison with other numerical analysis techniques, ANN has notable benefits such as learning ability and generalization, tolerance to errors and low computational cost [8]. Despite its many benefits, ANN suffers from a number of restrictions in the learning procedure, which mainly conducted by back-propagation (BP) algorithm, such as optimal adjusting of neurons connection weights and uncertainty of global minimum convergence. The mentioned inherent drawbacks can be modified by particle swarm optimization algorithm to deal with complicated nonlinear problems. Compared to the GA (genetic algorithm), PSO has advantages such as easy implementation, low parameters, and high convergence rate. The main objective of the PSO algorithm application is to optimize ANN neuron interconnection weights and bias to improve its performance for leaching process modeling.

For the sake of popularization, there is an extensive desire for ANN methods, e.g., theoretical analytical and pharmaceutical chemistry, biochemistry, food and management of waste disposal [9–12]. The ability of ANN in the evaluation of quantitative chemico-physical parameters as well as metals recovery optimization in extractive metallurgy with some advantages over conventional parametric approaches was validated [13–15]. The combined evolutionary methods (i.e. PSO–ANN) has been applied to model nonlinear relationship between the photocatalytic degradation reactivity of beta-naphthol on the titanium dioxide (TiO_2) nanoparticles [16], to predict the flashpoints of organic compounds [17], to estimate the compressive strength of rock [18], classification of black plastic types [19] and to predict the separation of zinc ions by activated carbon from aqueous environment [20]. Particle swarm optimization and neural network methods were also used to optimize the performance of lithium-ion batteries and to investigate leaching processes. For instance, Sun et al. [21] employed particle swarm algorithm to optimize the Levenberg–Marquardt neural network topology to evaluate the state of charge (SOC) of lithium-ion batteries. Moreover, Khajeh et al. [22] utilized the combination of particle swarm optimization and ANN to evaluate the optimum behavior of leaching—liquid/liquid microextraction of zinc from flour and found out that the model can be applied to estimate the Zn extraction efficiency by a relative standard deviation error (RSD%) less than 4%. The ability of PSO–ANN to estimate the water amount of natural gas (sour and sweet) has been confirmed for wide ranges of CO_2 and H_2S contents, temperature, and pressure [23]. Additionally, the satisfactory results of PSO coupled ANN in estimating the molybdenum extraction efficiency in water samples using morin-stabilized silver nanoparticles shows another evidence of its applicability in the modeling of various processes [24]. The performance of PSO–ANN in the prediction of chemico-physical processes characteristics is in some cases acceptable [25–29] and thus, the technique can be employed to the comprehensive analysis and modeling of the leaching processes.

To achieve optimal recovery conditions the ANN modeling of waste LIBs leaching process has significant importance. In the recent study, the capability of PSO–ANN technique evaluated for prediction of the cobalt leaching percentage from the spent lithium-ion batteries through H_2SO_4 and H_2O_2 mixture. According to the literature, so far the leaching of cobalt from spent LIBs has not been studied using PSO–ANN technique. To determine the dependency of the cobalt leaching on the reaction parameters, i.e., reagents concentration, leaching solution pulp density, temperature and reaction time, 42 repeatable numerous leaching tests are performed using spent LIBs cathodic materials. The leaching dataset used to train and validate 10 models with different structures and the predictability of three reliable models was evaluated using statistical measurements. Pursuant to the PSO–ANN model results, it will be shown that the prediction of leaching reaction in terms of operational parameters can be achieved with high accuracy.

Experimental and theoretical aspects

Materials and leaching experiments

Various brands of spent LIBs used in cell phones were completely discharged in 5% NaCl solution for 24 h and dismantled manually and the plastics, cathodes, anodes, and cell cases separated from the batteries [5, 30]. Then, the electrodes containing cathodic material was treated using *N*-methylpyrrolidone (NMP) for 1 h at 70 °C. Once purification, the obtained materials dried for 24 h at 100 °C and heated at 700 °C for 5 h in a muffle furnace to remove carbon, PVDF (polyvinylidene fluoride) and NMP excess present in the powder. The resulted powder was ground and sieved with the 0.5 mm screen. All the leaching processes were performed in a 0.5 L three-necked reactor equipped with the condenser and thermometer. First, 3 gr

cathodic materials of spent LIBs mixed with H_2SO_4 (Merck, 95–97.0%) solution and after the thermal equilibrium establishment, the hydrogen peroxide (H_2O_2, Sigma-Aldrich 30%) was added to the reactor. In each leaching test, the reaction solution samples were taken at certain intervals to analysis of cobalt ion content. Table 1 shows the leaching parameters range with optimal reaction conditions [31].

Training of artificial neural network and particle swarm optimization for cobalt leaching

Artificial neural network

ANNs are computing units inspired by the biological complex neural structures. They are used extensively in data classification, function estimation, and signal analysis. Neurons link to each other by some weight coefficient, i.e., the strength of the connection and each neuron consists of its own activation function, input and output. One of the most popular ANN networks is multilayer perceptron (MLP) neural networks. In the ANN structure, Inputs and outputs are directly related to the input and output layers, respectively. The hidden layers are placed between the input and output layers. The transformation of information from the one layer's neuron to the other neuron of the subsequent layer conducted in the base of the following relationship:

$$y = \zeta(s) = \zeta\left(b + \sum_{i=1}^{n} w_i x_i\right) \quad (1)$$

where x_i is the input, $\mathbf{b}$ is the bias, $\mathbf{w_i}$ is the weight of neurons connection, s the activity, $\boldsymbol{\zeta}$ the activation or transfer function and y is the output of the neuron. The multilayer perceptron (MLP) training or learning step accomplished by iterative weighing procedures from the inputs to the outputs neurons which are called epochs. After each iteration, the evaluated outputs compare with the real ones (targets) in the base of mean squared error (MSE) or other statistical measure criteria. In this process the weights and bias modified according to the learning algorithm, such as back-propagation, to minimize the MSE in each epoch. The configuration of the neural network includes the neurons number in input, hidden and output layers, connection weights and transfer functions optimized in a way in which the global minimum is achieved. After the training phase, in order to verification of process, the validation and testing phases performed with previously unused data in the training step, randomly.

Table 1 Spent LIBs leaching experimental conditions

Leaching parameter	Value
Sulfuric acid/M	1–4 (**2**)
H_2O_2/Vol%	0–5 (**4**)
Temperature/ °C	20–80 (**70**)[‡]
Reaction time/min	1–135 (**120**)
Pulp density (g/L)	40–180 (**100**)

Bold numbers correspond to the optimal values of the reaction parameters

[‡]Optimum value

The most important reaction parameters of the leaching process that affect the cobalt recovery efficiency from spent LIBs cathodic materials are reagents concentration (sulfuric acid (H_2SO_4) and hydrogen peroxide (H_2O_2)), leaching solution pulp density ($\rho_{S/L}$), reaction time (τ_r) and temperature (T_r). The dependence of the cobalt recovery efficiency on the leaching reaction key parameters can be shown as below [32]:

$$\psi_{Co} = f\left(C_{H_2SO_4},\ \mathrm{Vol}\%_{H_2O_2},\ T_r,\ \tau_r,\ \rho_{S/L}\right) \quad (2)$$

Since the rate of leaching solution stirring had the least effect on the cobalt recovery efficiency, hence, the optimum value (rpm = 300) of this parameter was fixed during all experiments and not considered in the data training process of the PSO–ANN models. The values of the leaching reaction parameters as model inputs along with extracted cobalt percentage from the spent LIBs in each leaching test are shown in Table 2. About 65% (27 samples) of the data set was employed in training phase, 16% (7 samples) in validation step and the remaining of them were used to test the output of the PSO-optimized ANN models for estimation of leached cobalt percentage, randomly. Normalization of dataset in the [0 1] interval was accomplished by means of the Eq. (3):

$$\psi_N = \frac{\psi - \psi_{\min}}{\psi_{\max} - \psi_{\min}} \quad (3)$$

where ψ, ψ_N, $\psi_{\min}$ and $\psi_{\max}$ are actual, normalized, minimum, and maximum of data values, correspondingly. Subsequently, the normalized data of leaching efficiency were investigated by denormalization of units.

Particle swarm optimization algorithm

The PSO algorithm starts by creating a random population. Each component in a population is a different decision variable whose optimal value must be determined and indeed each particle represents a vector in the problem-solving space. In this algorithm, any component action affects the movement of the group, and eventually, each member of the group can benefit from the discoveries and skills of other members.

The fundamental difference between PSO and other optimization algorithms is the velocity vector that forces the members of the set to change the position in the search space (Fig. 1). This velocity vector resultant from the p and p_g

Table 2 The experimental dataset used in PSO–ANN modeling

No.	Inputs					Output
	H_2SO_4 (mol $L^{-1)}$	H_2O_2 (Vol%)	Reaction time (min)	Temperature (°C)	$\rho_{S/L}$ (g/L)	Leaching efficiency (%)
1	1	4	120	70	100	17.68
2	1.5	4	120	70	100	65.05
3	2	4	120	45	100	65.7
4	1.75	4	120	70	100	83.9
5	**2**	**4**	**120**	**70**	**100**	**99.77**
6	2.25	4	120	70	100	98.34
7	2.5	4	120	70	100	97.3
8	2.75	4	120	70	100	98.48
9	3	4	120	70	100	99.78
10	3.5	4	120	70	100	98.69
11	4	4	120	70	100	97.25
12	2	0	120	70	100	27.49
13	2	0.5	120	70	100	42.86
14	2	1	120	70	100	57.17
15	2	2	120	70	100	76.83
16	2	3	120	70	100	88.81
17	2	4	120	70	100	99.04
18	2	5	120	70	100	97.27
19	2	4	15	70	100	33.95
20	2	4	30	70	100	68.5
21	2	4	60	70	100	98.63
22	2	4	75	70	100	98.39
23	2	4	90	70	100	99
24	2	4	135	70	100	93.86
25	2	4	120	20	100	29.96
26	2	4	120	25	100	38.83
27	2	4	120	35	100	52.68
28	2	4	120	50	100	82.46
29	2	4	120	60	100	94.37
30	2	4	120	70	100	98.15
31	2	4	120	80	100	98.72
32	2	4	120	70	40	27.03
33	2	4	120	70	50	36.86
34	2	4	120	70	60	43.55
35	2	4	120	70	70	56.46
36	2	4	120	70	80	78.8
37	2	4	120	70	90	88.35
38	2	4	120	70	110	98.66
39	2	4	120	70	120	98.5
40	2	4	120	70	140	98.45
41	2	4	120	70	180	92.27
42	2	4	45	70	100	93.04

Bold numbers correspond to the optimal values of the reaction parameters

vectors. P is the best position where a certain particle has reached and p_g is the optimized position at which the best particle in the vicinity of that particle has already reached and consequently, the process provides a solution in each iteration. In the d-dimensional search space, the particle **i** is indicated by a k-dimensional position vector ($X_i = (X_{i1}$,

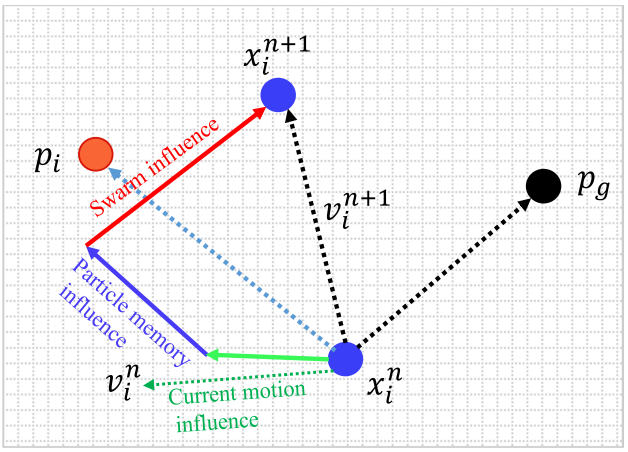

Fig. 1 Searching concept with particles in a solution space

$X_{i2},\ldots,X_{ik}$), k-dimensional velocity vector ($V_i = V_{i1}$, $V_{i2},\ldots,V_{ik}$), the best position found by a given particle ($P_{i,\,\text{best}} = (p_{i1}, p_{i2},\ldots,p_{ik})$ and the best position which find with the best particle among the whole particles ($P_{g,\,\text{best}} = (p_{g1}, p_{g2},\ldots,p_{gk})$. Eventually, the population purposefully moves to the optimal point using the following relationships:

$$x_{ik}^{n+1} = x_{ik}^{n} + v_{ik}^{n+1} \tag{4}$$

$$V_{ik}^{n+1} = \omega.v_{ik}^{n} + c_1 r_1^n \left(p_{i,\,\textbf{best}}^n - x_{ik}^n\right) + c_2 r_{ik}^n \left(p_{g,\,\textbf{best}}^n - x_{ik}^n\right) \tag{5}$$

In the above relations, **ω** is the inertia factor, which is used for evaluation of the performance and convergence rate. The r_1 and r_2 are random numbers, i.e., the normal distribution in [0 1] interval. **n** is the number of iteration, c_1 is the cognitive component, i.e., the best situation that a member gained, and c_2 is the social component, i.e., the best situation that detected by the entire group. PSO–ANN optimize the connection weights and biases of the neural network. The neural network model structure used in spent LIBs leaching evaluation is shown in Fig. 2.

Structural optimization of PSO–ANN was obtained according to the maximum and minimum values of R^2 and MSE, respectively. In this method, firstly N position vectors are generated randomly, and then the neural network is executed with these vector parameters and consequently, the error resulting from each run is considered as the fitness condition of that network variable vector. This process iterated until the final convergence is obtained, i.e., the optimal position vector (optimal network bias and weights values, Fig. 3) in which the training error is minimal. The values of c_1 and c_2 (Eq. 5), the number of particles, and the maximum number of iterations was selected 2, 2, 20 and 100, respectively.

Comparison of PSO–ANN models performance evaluated by statistical quality criteria: R^2 (the correlation coefficient), MAE (mean absolute error), MSE (mean squared error), RRSE (root relative squared error) and RMSE (root mean square error):

$$R^2 = 1 - \frac{\sum_{i=1}^{N} (\psi_i^{\exp} - \psi_i^{pred})^2}{\sum_{i=1}^{N} (\psi_i^{pred})^2} \tag{6}$$

$$MAE = \frac{1}{n} \sum_{i=1}^{N} \left| \psi_i^{\exp} - \psi_i^{pred} \right| \tag{7}$$

$$MSE = \frac{1}{n} \sum_{i=1}^{N} \left| \left(\psi_i^{\exp} - \psi_i^{pred} \right)^2 \right| \tag{8}$$

$$RRSE = \left(\frac{\sum_{i=1}^{N} (\psi_i^{\exp} - \psi_i^{pred})^2}{\sum_{i=1}^{N} (\psi_i^{\exp} - {}^1\!/_n \sum_{i=1}^{N} \psi_i^{\exp})^2} \right)^{0.5} \tag{9}$$

$$RMSE = \left(\frac{1}{n} \sum_{i=1}^{N} \left(\psi_i^{\exp} - \psi_i^{pred} \right)^2 \right)^{0.5} \tag{10}$$

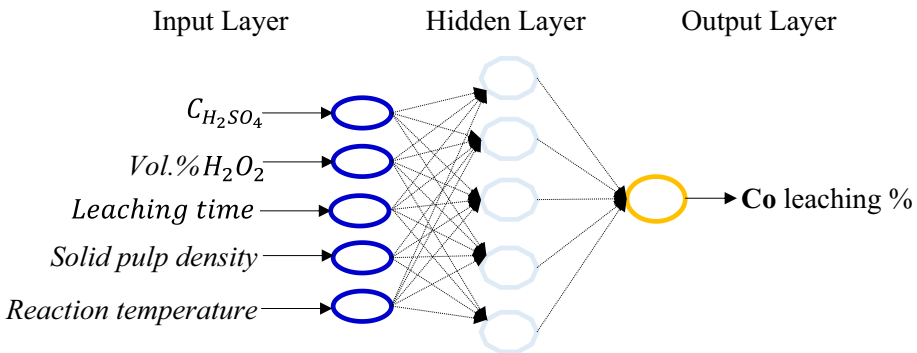

Fig. 2 Three layer feed-forward ANN training for prediction of spent LIBs leaching efficiency

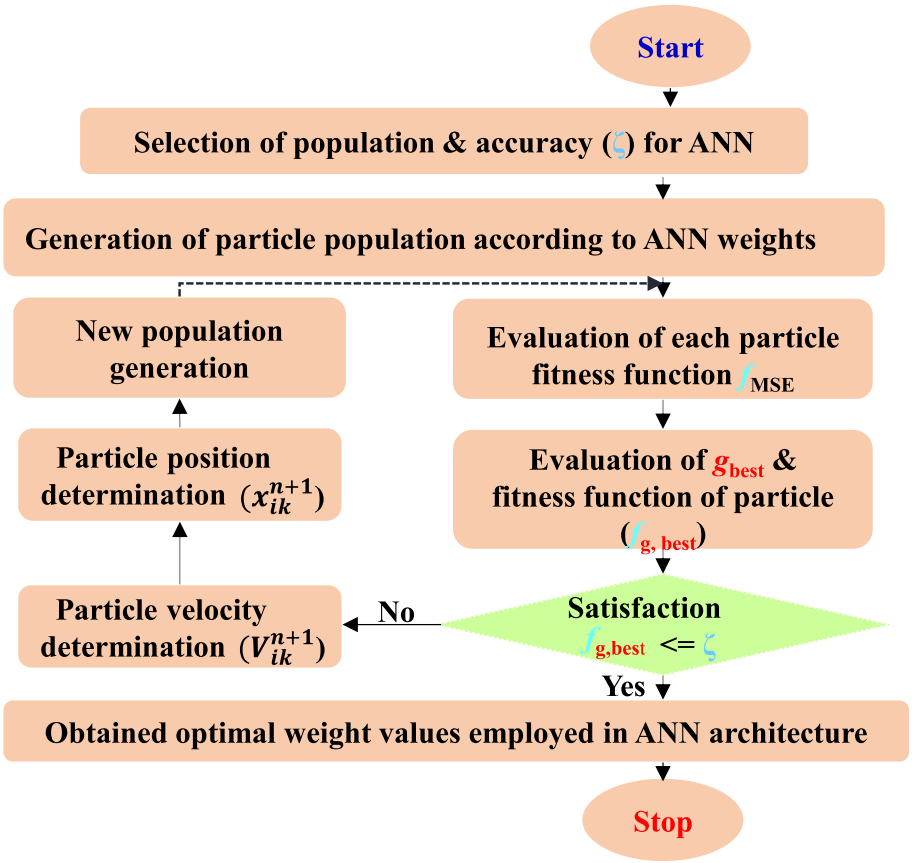

Fig. 3 Optimization of ANN architecture using the PSO algorithm for leaching reaction prediction of spent LIBs

which, ψ_i^{exp} is the experimental (target) value, ψ_i^{pred} is the model predicted value and **n** is the data set number in the training and testing stages of each model.

Results and discussion

The main metals recovery efficiency of the spent LIBs is a function of leaching process parameters. By evaluating the leached percentage of cobalt, it is possible to predict the amount of LIBs recovery in different operating conditions. Figure 4 shows the advancement of modeling by the PSO algorithm in the training phase in the base of layer weights and fitness value trend. The figure represents the optimized progress for the different neuron numbers and excitation functions. Root mean square error (MSE) has been used as the statistical measure for determination of the optimal PSO–ANN model. The fitness value (MSE) in each model pursuant to different activation functions and neurons number (Table 3) indicated in Fig. 4.

By changing the generation number, the improvement of the process will happen. Therefore, after the sufficient process iteration, the error values will decrease and the optimized solution can be chosen. The fitness value decrease trend remained until the defined 100 generations

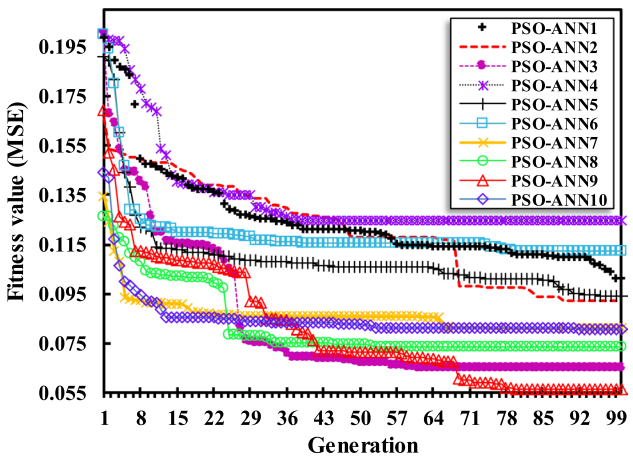

Fig. 4 Fitness value of training procedures at the different number of neurons and activation functions

for PSO–ANN models design are achieved. As shown in Fig. 4 by proper selection of generation amount there is no further change in error values after multiple iterations. Therefore, the optimum 100 generations number, by considering the calculation cost, was chosen for PSO–ANN models. In the base of Fig. 4, averagely, the Tangsig

Table 3 The results of statistical measurements of the PSO–ANN model accuracy at different Configurations

ANN configuration			Statistical measurements			
Model	Function	Neurons*	R^2	MSE	RRSE	MAE
PSO–ANN1	Logsig–Purelin	7	0.931	0.144	0.272	2.326
PSO–ANN2	Tangsig–Purelin	4	0.973	0.109	0.201	3.756
PSO–ANN3	Tangsig–Purelin	8	0.985	0.060	0.139	2.262
PSO–ANN4	Logsig–Purelin	3	0.907	0.139	0.149	2.812
PSO–ANN5	Logsig–Purelin	14	0.960	0.104	0.315	4.434
PSO–ANN6	Tangsig–Purelin	12	0.959	0.122	0.223	6.383
PSO–ANN7	Logsig–Purelin	17	0.983	0.089	0.310	2.607
PSO–ANN8	Logsig–Purelin	28	0.984	0.070	0.201	2.878
PSO–ANN9	Tangsig–Purelin	25	0.985	0.069	0.153	2.683
PSO–ANN10	Logsig–Purelin	16	0.975	0.077	0.145	2.597

*Hidden layer

activation function (Table 3) has the preferable efficiency to elect the proper weights of model layers.

To evaluate the modeling procedure and measuring the effect of functions on the PSO–ANN optimization, the MSE as fitness criteria for each model has been presented in Fig. 5b. The model with MSE value closer to zero has the better performance within the proposed models. According to the average values of MSE for employed activating functions, the Tangsig for 4 selected models by an average of 0.090 has better performance compared with the Logsig function for 6 selected models by an average of 0.103. As seen in Fig. 5b the number of neurons do not follow a specific evolution trend and generally MSE decrease with neurons number. Therefore, it can be stated that the desired performance can be obtained by random progress.

The selection of the proper model among the proposed models can be accomplished in the base of other statistical measurements. For this purpose, the statistical criteria for

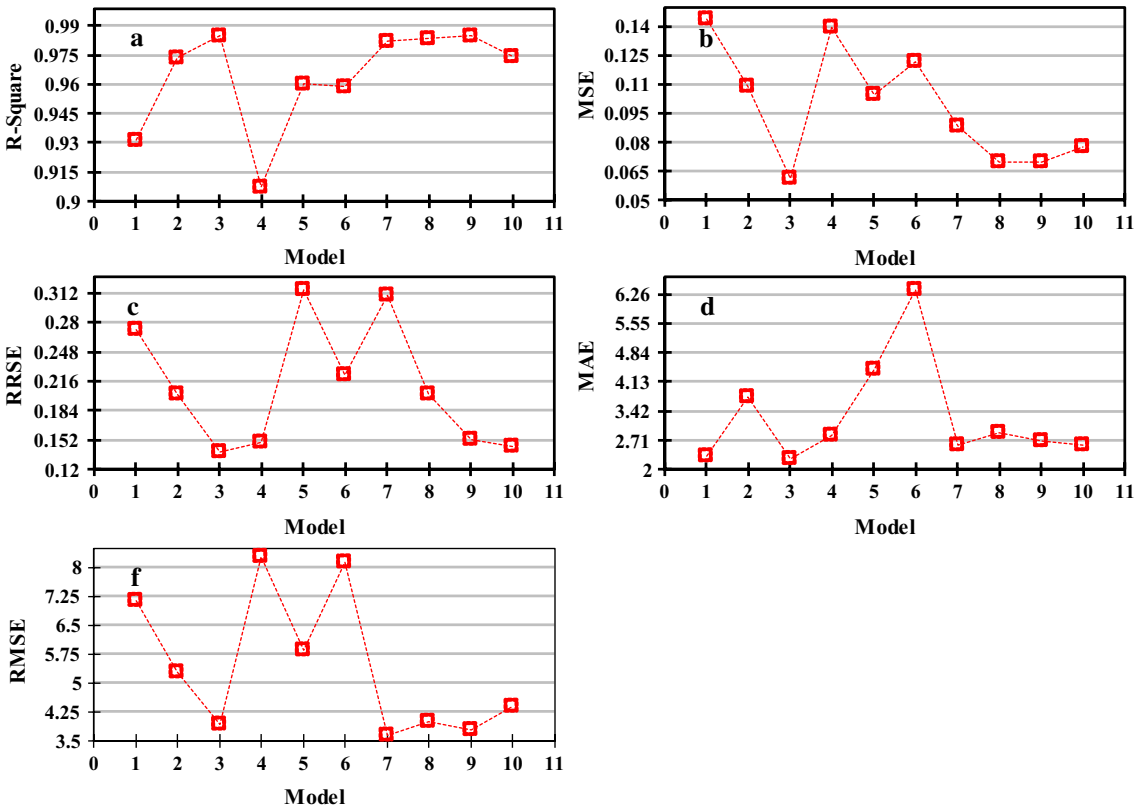

Fig. 5 Statistical measures in PSO–ANN models **a** R-square, **b** MSE, **c** RRSE, **d** MAE, and **f** RMSE

each PSO–ANN model have been presented in Fig. 5. From part c of Fig. 5, the value of RRSE measures for Tangsig and Logsig functions with different neurons number are under the 0.28 and 0.312, respectively. Indeed, the RRSE measure near to zero indicates the best functionality of the proposed model. Model PSO–ANN3 with 0.139 RRSE value is the best model within the proposed models. The analysis of R^2 measure that is shown in part **a**, according to the accuracy and performance of selected models, showed that the PSO–ANN3 with 0.985 value has the best performance. In the base of *R*-square scale, the models by value near the 1 have high performance. Also, based on the MAE criterion (Fig. 5d), model 3 with an average absolute error value of 2.02 represents the best model to evaluate the amount of cobalt leaching from the spent LIBs.

The accuracy of ANN is verified with the ability of the model for prediction of sample data with an acceptable error. Figure 6 shows the predicted cobalt leaching efficiency from the spent LIBs in different reaction conditions. The models with Tangsig function and different neurons number (models 2 and 3 in Fig. 6a and models 8 and 9 in Fig. 6b) have better prediction accuracy in comparison with Logsig function.

Comparison the experimental and predicted values of the cobalt leaching percentage from the cathodic materials of spent LIBs for the ANN (with 3 neurons in hidden layer and *Levenberg–Marquardt* training function), PSO–ANN3, PSO–ANN8 and PSO–ANN9 models (through the training and testing steps) via linear fitting line, its function and the *R*-square values shown in Fig. 7.

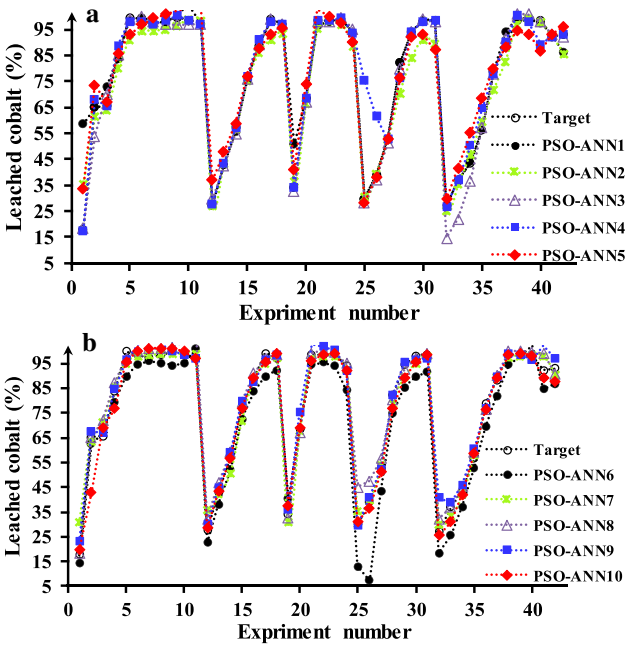

Fig. 6 The output of PSO–ANN models for leached cobalt percentage **a** PSO–ANN#1-5 and **b** PSO–ANN#6-10

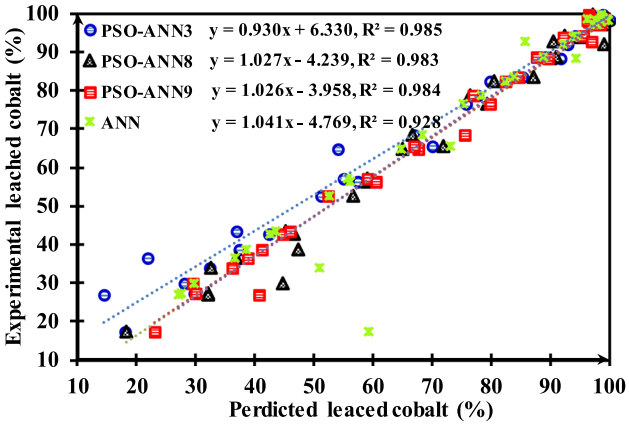

Fig. 7 Experimented versus predicted leached cobalt percentage through the ANN, PSO–ANN3, PSO–ANN8 and PSO–ANN9 models

As shown, there is good compatibility between the experimental and the data obtained from the output of the three PSO–ANN models while some output data of the ANN model are scattered from the baseline. To further analyze and compare the performances of two methods considered in this paper the hypothesis Wilcoxon test and error test are also carried out. The error test results are drawn using box plots in Fig. 8. In the figure, the rectangles and the black line between them show the second and third quarter and the mean value of errors, respectively. The maximum and minimum values are presented as error bars on the sides of the rectangles. It can be seen that the distribution of errors around the median in both methods is almost asymmetric. However, the distance between the minimum and maximum of uncoupled ANN model errors are larger than the PSO–ANN models which impose limits on the predictability of the not optimized ANN models by overshooting. According to the *p* value of the Wilcoxon hypothesis test (Fig. 8), it is obvious that ANN with PSO trained gives the better result and performance compare to ANN. Moreover, pursuant to the statistical criterion of MSE, all of PSO–ANN models compared to the ANN model show a high degree of reliability in predicting the amount of cobalt dissolution in the leaching process. In other side, PSO-coupled neural networks have higher R^2 compared to the uncoupled ANN. Also, the statistical fitness between simulated and predicted data shows that the PSO–ANN3 is more accurate than ANN in both training and testing stages. The values of R^2, MAE, MSE and RMSE for PSO–ANN3 (Fig. 5a, b, d, f) were 0.985, 2.02, 0.061 and 3.91 and for ANN were 0.928, 2.43, 0.365 and 7.28, respectively. It can be concluded that the optimization of neuron interconnection weights and the ANN bias with PSO algorithm has added the ability of model prediction. The output values from the PSO–ANN3 model are very close to the experimental values and the present model

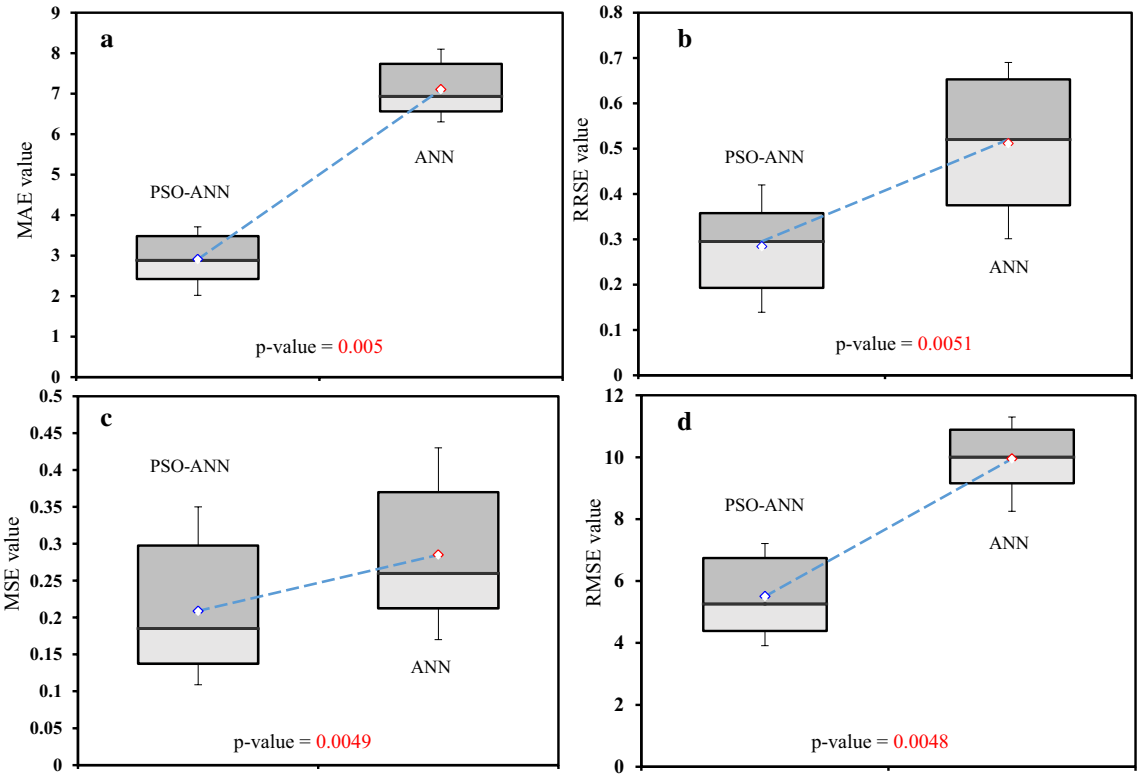

Fig. 8 Boxplots of errors in PSO–ANN and ANN models with p-values of two-sided Wilcoxon test (hypothesis {H_0: PSO–ANN median = ANN median Or H_A: PSO–ANN median < ANN median}): **a** MAE, **b** RRSE, **c** MSE and **d** RMSE

has the ability to predict the cobalt leaching rates under the experimental conditions. Therefore, the PSO–ANN3 model has the highest accuracy among the available models in the cobalt leaching process modeling and selected as the most suitable model in this study. According to the PSO–ANN leaching modeling results and under the optimum practical conditions of leaching ($C_{H_2So_4}$ = 2 mol/L, Vol% $_{H_2O_2}$ = 4, S/L = 100 gr/L, T = 70 °C, t = 120 min) the maximum amount of cobalt can be extracted.

Sensitivity analysis, evaluated from the effect of ± 10% changes in the reaction parameters value on the cobalt leaching efficiency, is applied to distinguish the influence of the reaction parameters on the spent LIBs cathodic materials leaching percentage. Since, PSO–ANN3 is the best model for evaluation of the leaching process, the recent model used for sensitivity analysis.

According to the leaching reaction parameters sensitivity analysis results (Fig. 9), the solid pulp density and the concentration of sulfuric acid have the most impact on the model performance while the remaining affect the model performance, slightly. It can be concluded that the $\rho_{S/L}$ and $C_{H_2So_4}$ are the most important components of the reaction. However, in some other reaction operating conditions the influence of the parameters on the leaching efficiency may be different. For instance, Gao et al. [33]

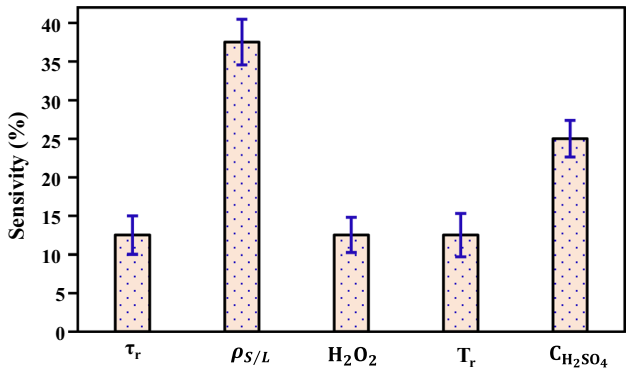

Fig. 9 Sensitivity analysis of spent LIBs leaching operative parameters

have stated that the type and concentration of acid are the most important parameters affecting spent LIBs leaching. Indeed, the mechanism of a certain leaching process can be unique owing to the different pre-treatment process of the cathodic powder, size and morphology of the reactive material particles, reagent type and their concentration, solution mixing speed and temperature. Hence, the influence and significance of the different parameters on the reaction progress, which appear in the rate equation in

some way [34], can change in accordance with the current conditions of the process.

Based on the chemical equation (Eq. 11), owing to the reactant apparent concentration increasing, as a result of $\rho_{S/L}$ increment, the amount of leaching efficiency increases until the leaching reaction equilibrium point ($S/L=\rho_{S/L}=100$ g/L, Table 1). In reality, the reaction efficiency depends on the solid-solution reaction rate and therefore to the reacted fraction of solid spent LIBs (S/L) as well as the leaching reagent concentration [35].

$$2LiCoO_2(s) + 3H_2SO_4(aq) + H_2O_2(aq) \rightarrow 2CoSO_4(aq) + Li_2SO_4(aq) + 4H_2O\,(l) + O_2(g) \quad (11)$$

At higher values of $\rho_{S/L}$, the leaching rate decreases probably due to the local depletion of leaching reagents in the vicinity of the solid particles for the sake of reaction solution viscosity and mass transfer limitation phenomena.

On the other hand, $C_{H_2So_4}$ is the other main parameters that affect cobalt leaching from the spent LIBs [31]. The cobalt leaching rate increases by increasing sulfuric acid concentration before the chemical reaction equilibrium point of the leaching process is attained (Fig. 10). Moreover, the dissolution of solid product(s) on the surface of the LIBs cathode materials, as a result of leaching reaction, accomplished by the sulfuric acid excess as the reaction proceeds within the leaching solution (Eq. 12). The recent functionality of sulfuric acid is essential to the leaching process progression. In other words, the rate of surface chemical reactions (include electron transfer) [34] is high consequently the cobalt ions concentration can be polarized in the vicinity of the cathodic material surface (saturation state). Therefore, it is a possibility of $Li_2Co(SO_4)_2$ nucleation on the reactive material surface (solid solution of the reaction (11) products) [36]. As well, the solid solution of the binary system (Li_2SO_4–$CoSO_4$, 1:1) is stable in agreement with the phase diagram and it can be formed at relatively low temperatures [37]. In the other hand, due to the kinetic conditions of the leaching system, the rate of formed nuclei ($Li_2Co(SO_4)_2$) dissolution can be higher than their growth rate. Therefore, it can be said that the complicated conversion of cobalt present in the cathode materials structure into the soluble ions accomplished as a result of sequential reactions (solid–liquid (11), nucleation and growth of the solid product, and dissolution (12)). Accordingly, the mechanism (shrinkage core model with surface chemical reaction controlling step) and the counter of the leaching reaction potential energy changes is shown schematically in Fig. 11.

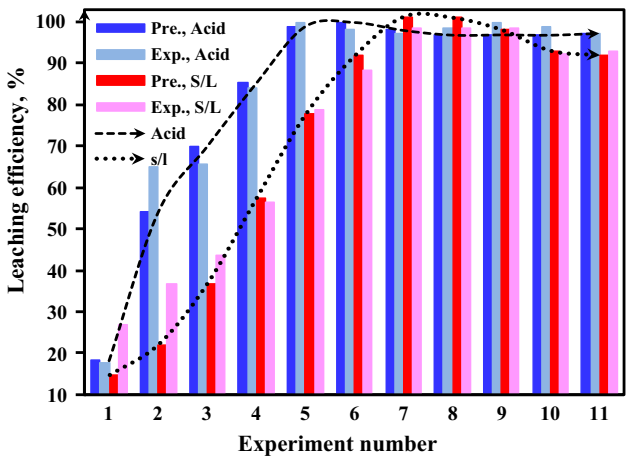

Fig. 10 Experimental (**Exp.**) and predicted (**Pre.**) data of cobalt leaching from spent LIBs at different sulfuric acid concentrations and solid/liquid ratios ($S/L=\rho_{S/L}$) (Tables 1, 2)

Given the above-mentioned mechanism, it can be concluded that the reaction (11) as the bottle-neck of the overall process has a significant contribution to the spent LIBs leaching. Eventually, by ignoring the transient state of binary product nucleation and considering the reaction rate coefficients difference ($k_{12} \gg k_{11}$), the overall reaction of the leaching can be summarized as a single-step process of Eq. (11).

In summary, the spent LIBs leaching reaction follows the shrinking core mechanism and contains the following steps [31]: (1)—adsorption and chemical reaction of the reagents mixture on the surface of spent LIBs cathodic materials, (2)—development of interphase reaction and production of solid products and (3)—dissolution of solid products at the reaction interface to form the soluble ions [38]:

$$Li_2Co(SO_4)_2(s) + 2H^+(aq) = 2Li^+(aq) + Co^{2+}(aq) + 2HSO_4^-(aq) \quad (12)$$

Due to the relatively low activation energy value (43–66 kJ mol^{-1}) [31, 39, 40], increasing the reaction temperature to the solution boiling point has a negligible influence on the reaction rate and thus on the leaching efficiency of cobalt. Therefore, the pulp density ($\rho_{S/L}$) and the concentration of sulfuric acid are the most effective parameters of the cobalt leaching from the spent LIBs under the reaction condition.

Conclusions

The hybrid of ANN and particle swarm optimization algorithm was implemented to estimate the cobalt leaching efficiency from the spent LIBs using H_2SO_4 and H_2O_2 mixture. The concentration of the reagents, pulp density, temperature and reaction time as inputs and leaching percentage of cobalt as output used for PSO–ANN modeling. Leaching modeling is carried by different activation functions and neuron

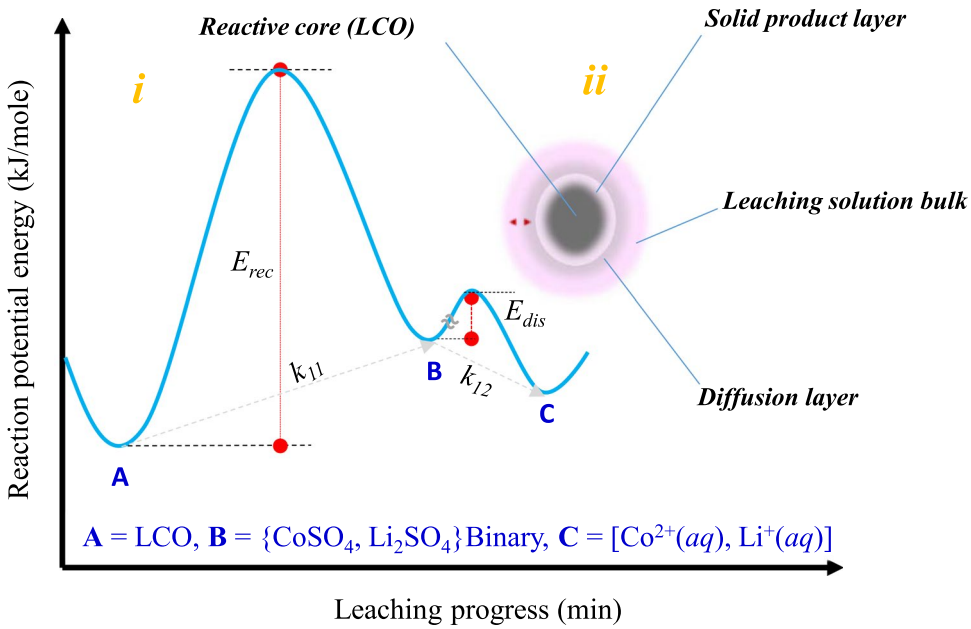

Fig. 11 Spent LIBs leaching progress: (i) potential energy changes (no scale) and (ii) the complex reaction mechanism, LCO = spent LIBs cathode materials, E_{rec} = chemical reaction activation energy, E_{dis} = dissolution activation energy, k_{11} and k_{12} are the related reaction rate coefficients

numbers. The performance and accuracy of the proposed approach validated by statistical measures of PSO–ANN model outputs. Comparing the values of predicted leaching efficiency with experimental data showed that the accuracy of PSO–ANN models is reliable. The best R^2 values for the data set was 0.985, with low errors rate, i.e., 0.06 and 0.139 for MSE and RRSE, respectively. Also, it was concluded that the pulp density ($\rho_{S/L}$) and H_2SO_4 concentration were the most important parameters of the leaching process. Using the proposed hybrid technique of artificial network and particle swarm optimization algorithm can assist to maximize the recovery of main metals in the practical process.

References

1. Zhang X, Xie Y, Lin X et al (2013) An overview on the processes and technologies for recycling cathodic active materials from spent lithium-ion batteries. J Mater Cycles Waste Manag 15:420–430
2. Zhang P, Yokoyama T, Itabashi O et al (1998) Hydrometallurgical process for recovery of metal values from spent lithium-ion secondary batteries. Hydrometallurgy 47:259–271
3. Dorella G, Mansur MB (2007) A study of the separation of cobalt from spent Li-ion battery residues. J Power Sources 170:210–215
4. Pant D, Dolker T (2017) Green and facile method for the recovery of spent lithium nickel manganese cobalt oxide (NMC) based lithium ion batteries. Waste Manag 60:689–695
5. Li L, Zhai L, Zhang X et al (2014) Recovery of valuable metals from spent lithium-ion batteries by ultrasonic-assisted leaching process. J Power Sources 262:380–385
6. Badawy SM, Nayl AA, El Khashab RA, El-Khateeb MA (2014) Cobalt separation from waste mobile phone batteries using selective precipitation and chelating resin. J Mater Cycles Waste Manag 16:739–746
7. Libraries T (2017) Sustainable recovery of cathode materials from spent lithium-ion batteries using lactic acid leaching system. ACS Sustain Chem Eng 5:5224–5233
8. Honório KM, De Lima EF, Quiles MG et al (2010) Artificial neural networks and the study of the psychoactivity of cannabinoid compounds. Chem Biol Drug Design 75:632–640
9. Marini F, Bucci R, Magrì AL, Magrì AD (2008) Artificial neural networks in chemometrics: History, examples and perspectives. Microchem J 88:178–185
10. Taylor P, Kundu P, Debsarkar A et al (2014) Artificial neural network modelling in biological removal of organic carbon and nitrogen for the treatment of slaughterhouse wastewater in a batch reactor. Environ Technol 35:1296–1306
11. Khataee A, Fathinia M, Rad TS (2016) Kinetic modeling of nalidixic acid degradation by clinoptilolite nanorod-catalyzed ozonation process. RSC Adv 6:44371–44382
12. Thakur V, Ramesh A (2018) Analyzing composition and generation rates of biomedical waste in selected hospitals of Uttarakhand, India. J Mater Cycles Waste Manag 20:877–890
13. Galván IM, Zaldívar JM, Hernández H, Molga E (1996) The use of neural networks for fitting complex kinetic data. Comput Chem Eng 20:1451–1465
14. Normandin A, Grandjean BPA, Thibault J (1993) PVT data analysis using neural network models. Ind Eng Chem Res 32:970–975
15. Aldrich C, Deventer J, Reuteri MA (1994) The application of neural nets in the metallurgical industry. Miner Eng 7:793–809
16. Ijadpanah-Saravi H, Safari M, Noruzi-Masir B et al (2017) Intelligent tools to model photocatalytic degradation of beta-naphtol by titanium dioxide nanoparticles. J Chemom 31:e2907
17. Lazzús JA (2010) Prediction of flash point temperature of organic compounds using a hybrid method of group contribution + neural network + particle swarm optimization. Chin J Chem Eng 18:817–823
18. Momeni E, Armaghani DJ, Hajihassani M (2015) Prediction of uniaxial compressive strength of rock samples using hybrid particle swarm optimization-based artificial neural networks. Measurement 60:50–63
19. Roh S-B, Oh S-K, Park E-K, Choi WZ (2017) Identification of black plastics realized with the aid of Raman spectroscopy and

fuzzy radial basis function neural networks classifier. J Mater Cycles Waste Manag 19:1093–1105
20. Rao R, Sahu JN (2018) Modeling and optimization by particle swarm embedded neural network for adsorption of zinc (II) by palm kernel shell based activated carbon from aqueous environment. J Environ Manag 206:178–191
21. Xia B, Cui D, Sun Z et al (2018) State of charge estimation of lithium-ion batteries using optimized Levenberg–Marquardt wavelet neural network. Energy 153:694–705
22. Khajeh M, Kaykhaii M, Hossein S, Shakeri M (2014) Particle swarm optimization—artificial neural network modeling and optimization of leachable zinc from flour samples by miniaturized homogenous liquid–liquid microextraction. J Food Compos Anal 33:32–38
23. Ahmadi M-A, Ahmad Z, Phung LTK et al (2016) Estimation of water content of natural gases using particle swarm optimization method. Pet Sci Technol 34:595–600
24. Khajeh M, Dastafkan K (2014) Removal of molybdenum using silver nanoparticles from water samples: particle swarm optimization–artificial neural network. J Ind Eng Chem 20:3014–3018
25. Ghaedi M, Ghaedi AM, Ansari A et al (2014) Artificial neural network and particle swarm optimization for removal of methyl orange by Gold nanoparticles loaded on activated carbon and Tamarisk. Spectrochim Acta Part A Mol Biomol Spectrosc 132:639–654
26. Sheikhan M, Pardis R, Gharavian D (2013) State of charge neural computational models for high energy density batteries in electric vehicles. Neural Comput Appl 22:1171–1180
27. Rahman A, Anwar S, Izadian A (2016) Electrochemical model parameter identification of a lithium-ion battery using particle swarm optimization method. J Power Sources 307:86–97
28. Agarwal S, Tyagi I, Kumar V et al (2016) Kinetics and thermodynamics of methyl orange adsorption from aqueous solutions—artificial neural network-particle swarm optimization modeling. J Mol Liquid 218:354–362
29. Mansouri I, Shahri A, Zahedifar H (2016) A new algorithm in nonlinear analysis of structures using particle swarm optimization. IIUM Eng J 17:157–168
30. Wang W-Y, Yen CH, Lin J-L, Xu R-B (2019) Recovery of high-purity metallic cobalt from lithium nickel manganese cobalt oxide (NMC)-type Li-ion battery. J Mater Cycles Waste Manag 21(2):300–307
31. Jha MK, Kumari A, Jha AK et al (2013) Recovery of lithium and cobalt from waste lithium ion batteries of mobile phone. Waste Manag 33:1890–1897
32. Joo S, Shin D, Oh C et al (2016) Selective extraction of nickel from cobalt, manganese and lithium in pretreated leach liquors of ternary cathode material of spent lithium-ion batteries using synergism caused by Versatic 10 acid and LIX 84-I. Hydrometallurgy 159:65–74
33. Gao W, Liu C, Cao H et al (2018) Comprehensive evaluation on effective leaching of critical metals from spent lithium-ion batteries. Waste Manag 75:477–485
34. Ebrahimzade H, Khayati GR, Schaffie M (2018) Leaching kinetics of valuable metals from waste Li-ion batteries using neural network approach. J Mater Cycles Waste Manag 20:2117–2129
35. Grenman H, Salmi T, Murzin DY (2011) Solid–liquid reaction kinetics—experimental aspects and model development. Rev Chem Eng 27:53–77
36. Meshram P, Abhilash A, Pandey BD et al (2019) Extraction of metals from spent lithium ion batteries—role of acid, reductant and process intensification in recycling. Indian J Chem Technol 25:368–375
37. Touboul M, Le Samedi E, Sephar N et al (1993) Binary systems with Li_2SO_4 as one of the components. J Therm Anal Calorim 40:1151–1156
38. Meshram P, Pandey BD, Mankhand TR, Deveci H (2016) Acid baking of spent lithium ion batteries for selective recovery of major metals: a two-step process. J Ind Eng Chem 43:117–126
39. Takacova Z, Havlik T, Kukurugya F, Orac D (2016) Cobalt and lithium recovery from active mass of spent Li-ion batteries : theoretical and experimental approach. Hydrometallurgy 163:9–17
40. He LP, Sun SY, Song XF, Yu JG (2017) Leaching process for recovering valuable metals from the $LiNi_{1/3}Co_{1/3}Mn_{1/3}O_2$ cathode of lithium-ion batteries. Waste Manag 64:171–181

Publisher's Note Springer Nature remains neutral with regard to jurisdictional claims in published maps and institutional affiliations.